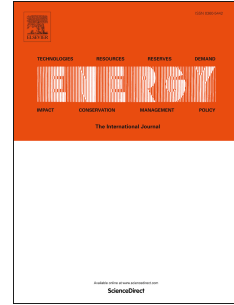


Journal Pre-proof

Economic performance evaluation of the wind supercharging solar chimney power plant combining desalination and waste heat after parameter optimization

Lu Zuo, Zihan Liu, Pengzhan Dai, Ning Qu, Ling Ding, Yuan Zheng, Yunting Ge



PII: S0360-5442(21)00745-3

DOI: <https://doi.org/10.1016/j.energy.2021.120496>

Reference: EGY 120496

To appear in: *Energy*

Received Date: 1 September 2020

Revised Date: 23 February 2021

Accepted Date: 25 March 2021

Please cite this article as: Zuo L, Liu Z, Dai P, Qu N, Ding L, Zheng Y, Ge Y, Economic performance evaluation of the wind supercharging solar chimney power plant combining desalination and waste heat after parameter optimization, *Energy*, <https://doi.org/10.1016/j.energy.2021.120496>.

This is a PDF file of an article that has undergone enhancements after acceptance, such as the addition of a cover page and metadata, and formatting for readability, but it is not yet the definitive version of record. This version will undergo additional copyediting, typesetting and review before it is published in its final form, but we are providing this version to give early visibility of the article. Please note that, during the production process, errors may be discovered which could affect the content, and all legal disclaimers that apply to the journal pertain.

© 2021 Published by Elsevier Ltd.

Economic performance evaluation of the wind supercharging solar chimney power plant combining desalination and waste heat after parameter optimization

Lu Zuo ^{a*}, Zihan Liu ^a, Pengzhan Dai ^a, Ning Qu ^a, Ling Ding ^a, Yuan Zheng ^a, Yunting Ge ^b

^a College of Energy and Electrical Engineering, Hohai University, Nanjing, 210098, China

^b Centre for Civil and Building Services Engineering, School of the Built Environment and Architecture, London South Bank University, London SE1 0AA, United Kingdom

Abstract: In this paper, the economic analysis model of solar chimney power plant combining seawater desalination and waste heat (SCPPDW) and wind supercharging solar chimney power plant combining seawater desalination and waste heat (WSCPPDW) was established. Based on net present value (NPV) method, the economic performance of two systems and that of WSCPPDW after optimization were studied. It was found that the addition of wind supercharging device increased the net income (NET) and NPV by 42.8% and 102.5%, respectively. With the increase of time, the annual NET of two systems increased, and the annual NPV firstly increased and then decreased. The annual NET and NPV of WSCPPDW were always larger than those of SCPPDW, which were negative in the first four years, but those of WSCPPDW were only negative in the first year. After sequentially optimizing the turbine rotational speed, nozzle length, chimney outlet radius and mixing section length, the power and freshwater output of WSCPPDW were improved by 455.8% and 11.7%, respectively. And the total net income (TNET) and total net present value (TNPV) were increased by 183.4% and 442.8%, respectively. The declining inflection point of annual NPV was brought forward by 10 years compared to that of initial WSCPPDW.

Keywords: Solar chimney power plant; Economic performance; Parameters optimization; Waste heat recovery; Desalination; Wind supercharging device

1 Introduction

1.1 Background

In order to deal with the energy crisis and fully make use of solar energy, the concept of solar chimney power plant (SCPP) was proposed [1–3]. It has a lot of outstanding advantages, such as single structure, low maintenance cost, wide source of construction material, reliable operation state and long-life cycle. A 50kW prototype SCPP was constructed in Manzanares (Spain) and connected to the grid, and it operated for 7 years since 1982 at an average of 8.9 hours per day under the supervision of one person [4,5]. The power output and system efficiency of the prototype SCPP were tested under different environmental conditions, which proved the economical reliability and utilization potential. However, because of the limitation of thermodynamic property, the air density difference between inside and outside the SCPP system was not significant, which resulted in low solar energy conversion efficiency. Besides, the multi-stage energy conversion process in SCPP system caused large energy loss. Therefore, the economic performance of prototype SCPP was relatively poor, considering its enormous dimensions (height of 194.6 m, heat collector radius of 122 m) [2,6].

Because of the shortcomings, including low solar energy conversion efficiency, large size of structure and high investment cost, the commercial application of SCPP technology is limited [7,8]. On the one hand, many researchers attempted to optimize the structural parameters of SCPP, including chimney height, heat collector radius and chimney radius, to improve the energy conversion efficiency [9,10]. On the other hand, combining SCPP technology with other technologies, such as seawater desalination [11–20], solar dryer [21], external heat sources [22–31], flat mirrors [32] and heat storage technology [33], is also a main development direction.

Combining solar desalination or external heat source has aroused many researchers' interests recently. Solar desalination is a good solution to deal with water crisis. Disc-type solar distiller, a relatively mature technology, is one of the most important solar desalination methods. Considering the fact that both of SCPP and

solar disc-type distiller occupy large land areas, many integrated SCPP systems combining desalination have been proposed to realize multi-object products output, including freshwater, power and raw salt, which is a beneficial way for improving solar energy utilization efficiency [12,16]. Besides, one of the most important challenges for SCPP application is the operation discontinuity at night and on rainy days [34]. Because of the continuous and relative high temperature of external source, coupling SCPP system with external heat source has potential to overcome the intermittency of electricity generation and realize the continuous work with considerable products output [17,35]. Both of combining SCPP system with desalination and external heat source are beneficial to promote the feasibility for developing SCPP technology.

1.2 Literature review of the economic performance of SCPP systems

The economic feasibility of SCPP system is crucial to its future development. Considering the low energy utilization efficiency and high investment cost, the power output will be considerable only when the sale reaches megawatt level with large structural size, high construction difficulty and expensive construction cost [6]. Many researchers have studied the economic feasibility of SCPP systems for contributing to the development and application of SCPP technology.

Schlaich [4] and Bernardes et al. [36] evaluated the cost of components in SCPP system with different size parameters, forecasted the levelized electricity price (LEC) of SCPP, and explored the LEC sensitivity to some important economic parameters. However, they didn't take the effect of carbon credit into consideration. Schlaich et al. [37] studied the economic feasibility of SCPP systems with different power capacity in Spain, and they concluded that with the improvement of power generation capacity, the LEC decreased. And the power capacity and LEC ranged from 5-200 MW and 0.21-0.74 €/kW, respectively. Nizetic et al. [38] took SCPP as an energy source of residents and island countries in Mediterranean area. A simplified model was developed to calculate the power output, investment cost and power consumption. It

was found that the power price of SCPP was higher than that of other power generation technologies. Zhou et al. [39] made some uncertain assumptions, considering interest rate, inflation rate, carbon credits, depreciation period, for comparing the cash flow of a 100 MW floating solar chimney power plant (FSCPP) with reinforced concrete solar chimney power plant (RCSCPP) and solar photovoltaic plant (SPVP). It was found that FSCPP had better economic feasibility than the other two systems with the same power capacity. Based on the SCPP proposed by Schlaich [4] and Bernardes et al. [36], Fluri et al. [40] developed a more detailed novel model to study the economic characteristics of SCPP. The results showed that the initial cost of large scale SCPP and LEC may be underestimated by using the previous models, and the carbon credit was able to reduce the LEC. Cao et al. [41] took Lanzhou city (China) as a hypothetical construction site. The economic performance of conventional solar chimney power plant (CSCPP) and sloped solar chimney power plant (SSCPP) were studied by comparatively analyzing their cash flow within the lifetime. It was found that the investment of SCPP was affected by its structure and material price, and the SSCPP was more cost-effective. Compared with traditional fossil fuel combustion plants, the SCPP with large power capacity was more competitive. Li et al. [42] analyzed the economic feasibility of a reinforced concrete SCPP in the northwest of China, using fixed assets evaluation model and risk-adjusted discount rate. The total net present value (NPV) and the lowest power prices in four operation stages were studied. It was concluded that the economic performance was superior between the second stage and the fourth stage. The total net present value was very sensitive to the change of solar electricity price and inflation rate, but the variations of carbon credits price, income tax rate and loan interest rate had little effect on the total net present value. Akhtar et al. [43] studied the economic feasibility of a 200 WM SCPP in India. They explored the effects of the interest rate, inflation rate and operation period on the LEC. Under the interest rate of 6%, the LEC was sensitive to the change of inflation rate. The LEC was reduced with the decrease of inflation rate and the

increase of working time. Gholamalizadeh et al. [44] introduced an optimization methodology for obtaining the optimal configuration (heat collector radius, chimney height and chimney radius) of SCPP, using a triple objective function covering power output, expenditure and total efficiency. Under the condition of optimal configuration, it was found that the benefit from increment of power output is higher than the expenditure. Okoye et al. [45] studied the feasibility of installing SCPP in the conditions of North Cyprus, and the most feasible cost option was determined by changing different parameters. It was found that the investment cost, plant capacity and chimney height were key parameters to evaluate the feasibility of SCPP. Then, Okoye et al. [46] conducted a feasibility study for SCPP system and proposed a novel method to determine the optimum SCPP dimensions and economic feasibility. It was found that the decreasing of discount rate and the increasing of collector and turbine efficiencies could improve NPV. Ali et al. [47] proposed a method for optimizing economic parameters of SCPP systems by comparing the actual achieved simple payback period and the minimum possible simple payback period. And twelve optimal models were established for studying SCPP systems with different design concepts, including reinforced concrete chimney, sloped collector and floating chimney, in the range of 5-200MW. It was found that under the same conditions of solar radiation and electricity price, the simple payback period of the 200 WM SCPP with sloped heat collector is similar to the 5 MW SCPP with floating chimney. Based on hourly meteorological data and soil heat storage, Guo et al. [48] proposed an unsteady theoretical model for studying the SCPP annual power output. They applied the cost-benefit model to study the levelized cost of electricity (LCOE) of a 10 MW SCPP in Yinchuan (China). It was found that the LCOE was 0.4178 yuan/kWh, which could compete with wind power and solar photovoltaic power considering Chinese concessional loan. Asayesh et al. [15] investigated a comprehensive SCPP system combining desalination using particle swarm optimization (PSO) algorithm and one-dimensional simulation code. The results showed that when the radius of

desalination area was 85-125 m, the economic performance of the integrated system was optimal. Jamali et al. [49] presented a new cooling method for the semi-transparent photovoltaic system using a solar chimney (STPV-SC), and the comprehensive economic assessment was carried out. The payback period and unit cost of power output were regarded as the main economic indicators. The effects of packing factor, chimney height and heat collector radius on power output and economic performance were studied. It was found that packing factor could optimize the economic performance. When the packing factor was in the range of 0.3-0.5, the payback period was lowest. Zuo et al. [50] evaluated the economic efficiency of a wind supercharged solar chimney power plant (WS-SCPP). The results showed that the economic performance of WS-SCPP was always better than that of SCPP under the same working conditions due to the supercharging effect contributed by wind supercharging device. The lowest electricity selling price was greatly lower than that of SCPP, with a decrease of 20.1%.

1.3 Objectives of this study

Wind supercharging solar chimney power plant combining seawater desalination and waste heat (WSCPPDW) is a multi-object system combining SCPP technology, seawater desalination, wind supercharging device and the recovery of waste heat discharged from traditional thermal plant [17]. According to previous studies, the effects of wind supercharging device, working parameters, structural dimensions and environmental conditions on the heat transfer and products output have been studied by mathematical model and 3D numerical simulation [17,35]. It has been proved that combining SCPP with the desalination and external heat source could greatly improve the power output, freshwater yield and comprehensive energy utilization efficiency, and the optimization of working and structural parameters of WSCPPDW contributed to the improvement of working performance. Therefore, WSCPPDW may have potential to provide a possibility for future development and application of SCPP technology.

Because the size dimensions of WSCPPDW are extremely large, the investment cost will be very huge resulting in low economic feasibility and great commercial application difficulty. However, the superiority of WSCPPDW performance were only presented in the improvement of products output and energy conversion efficiency which could not directly reflect the advantages of economic advantages of WCPPDW. This research mainly focused on the benefit and cost study of the solar chimney power plant combing seawater desalination and waste heat (SCPPDW) and WSCPPDW. Given various income sources (electricity, carbon credit, freshwater and raw salt) and different kinds of costs (construction cost, interest, tax, insurance cost, operation and maintenance cost), the economic analysis model was developed by using NPV and risk adjusted discount rate methods, which took working time and risk value into account. Based on previous study, the economic analysis was carried out to further investigate the superiority of the optimal WSCPPDW. The influences of adding additional wind supercharging device at chimney outlet and the optimization of different parameters, including turbine rotational speed, nozzle length, chimney outlet radius and mixing section length, on the economic performance of WSCPPDW were explored.

This paper is organized as follow: the structure of WSCPPDW is described in Section 2; the mathematical models of income and cost analyses are presented in Section 3 and 4; the criterion of economic performance assessment is presented in Section 5; the economic benefit analyses after adding wind supercharging device and optimizing working and structural parameters are discussed in Section 6; finally, the conclusions are included in Section 7.

2 Physical model

SCPPDW and WSCPPDW are two integrated systems which combine with waste heat recovery technology, and they are the extended systems of the solar chimney power plant combined with seawater desalination (SCPPCSD) and wind

supercharged solar chimney power plant combined with seawater desalination (WSSCPPCSD), respectively [17,35]. Because the main difference between SCPPDW and WSCPPDW is the wind supercharging device installed at the chimney outlet, the following focuses on the working principle of WSCPPDW.

Fig.1 is the structure and schematic diagram of WSCPPDW [17]. As shown in Fig.1, WSCPPDW mainly consists of 6 parts, including spiral exhaust gas heating channel (SGC), close-type seawater distillation tank, heat collector, air turbine, common chimney of SCPP and thermal power plant, and wind supercharging device. The differences between WSCPPDW and WSSCPPCSD are the SGC and common chimney.

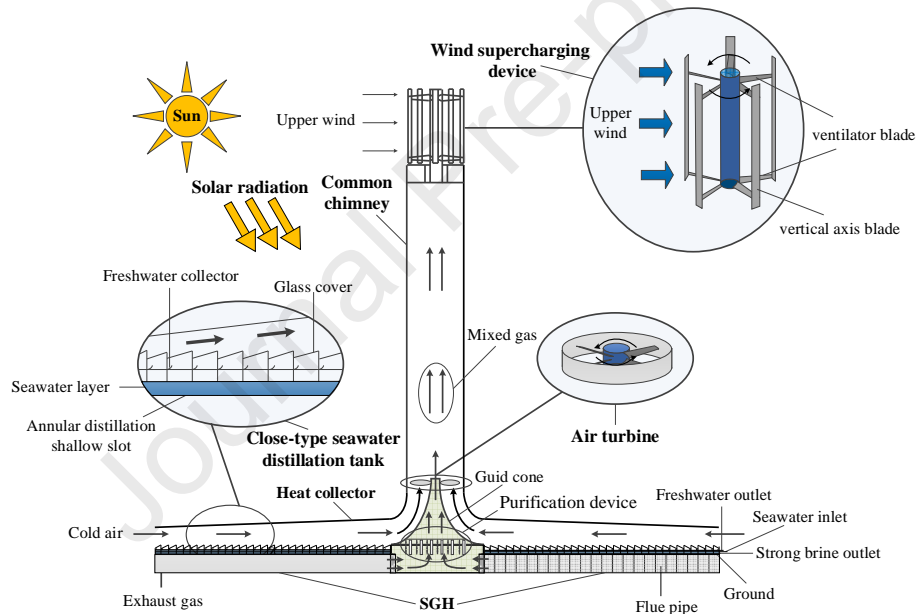


Fig.1 Structure and schematic diagram of WSCPPDW.

After being reheated by GGH (gas-gas heater) of thermal power plant, the flue gas enters the SGC arranged in spiral shape to heat the seawater in distillation tank. The seawater could store solar radiation energy and the energy of flue gas waste heat could ensure the continuous and stable operation state of WSCPPDW. The waste heat of flue gas greatly increases the seawater temperature, the evaporation capacity of seawater and the temperature of hot airflow in heat collector, which further improve the freshwater output. The flue gas flows through the SGC, and then enters the guide

cone cavity. In order to prevent the flue gas from corroding the inner wall of chimney and turbine blades, the flue gas is purified by the purification device (wet dust separator or other devices). The purified flue gas is injected into the common chimney by the nozzle at the outlet of guide cone. At the base of the common chimney, the high-speed flue gas jet flow generates vacuum effect and entrains its surrounding airflow. The mixture of high temperature flue gas and hot airflow increases the mass flow rate and temperature rise of airflow in WSCPPDW. Therefore, the turbine pressure drop and power output of the integrated system are both improved.

WSCPPDW utilizes different kinds of energy simultaneously, including wind energy, solar energy and flue gas waste heat energy, which improves the energy comprehensive utilization efficiency. The recovery of flue gas waste heat makes the system work continuously under the conditions of low solar radiation and night and improve the electricity output. The chimney in WSCPPDW is common chimney of SCPP and thermal power plant, that is, the high temperature flue gas from thermal power plant is discharged through the solar chimney, which greatly reduces the investment cost of construction.

Based on the dimension parameters of the prototype SCPP in Spanish Manzanares [2,3], some key parameters of WSCPPDW are shown in Table 1.

Table 1 Main dimension parameters of WSCPPDW.

Parameters	Values
Chimney height	194.6 m
Chimney radius	5.08 m
Collector radius	122 m
Collector height	1.85 m
Gas inlet temperature	358.15 K
Gas mass flow	436.3 kg/s
Environment temperature	298.15 K
Air inlet temperature	298.15 K
Environment wind velocity	2.5 m/s
Solar irradiance	850 W/m ²

3 Mathematical model of income analysis

On the one hand, combining with SCPP technology and solar disc-type seawater desalination technology, WSCPPDW economizes large land resource and construction cost. On the other hand, combining thermal power plant chimney and SCPP chimney reduces the construction cost. Therefore, WSCPPDW integrates many technologies which reduce the investment cost, realize the output of multi-object products, and greatly improve the system income. This paper analyzes the economic income of WSCPPDW. Its sources of profit consist of power output, carbon credit income, freshwater production and raw salt output.

3.1 Electricity income

This paper focuses on studying the economic performance of SCPPDW and WSCPPDW taking account of the influence of inflation rate on electricity price. Because the power consumption of WSCPPDW itself accounts for a very low proportion of its total power output, it is assumed that all the power output generated by WSCPPDW will be sold to electric power company. The economic performance is predicted based on the operation time of 8.9 h/day [4]. The electricity income of the k -th year of WSCPPDW can be expressed as follows:

$$B_p^k = E_p P_p (1 + \theta)^{k-1} \quad (1)$$

$$E_p = 3248.5 P_{sys} \quad (2)$$

$$0 \leq k \leq m \quad (3)$$

Where, E_p is the annual power output; P_p is the electricity unit price; θ is the constant inflation rate; m is the period of repaying the integrated system loan, $m=30$ [42].

3.2 Carbon credit income

WSCPPDW combines the chimneys of thermal power plant and SCPP, which saves the construction cost. Because WSCPPDW recovers the flue gas discharged

from thermal power plant for power generation, it has carbon credit income. If the difference between the flue gas discharged from WSCPPDW and thermal plant is ignored, the carbon credit income of WSCPPDW in the k-th year can be expressed as follows:

$$B_{co_2}^k = M_{co_2} E_p P_{co_2} (1 + \theta)^{k-1} \quad (4)$$

Where, M_{co_2} is the carbon emission of traditional thermal power plant; P_{co_2} is the carbon credit price.

3.3 Freshwater income

WSCPPDW can realize the joint production of freshwater and electricity, and its freshwater income in the k-th year is as follows:

$$B_w^k = E_w P_w (1 + \theta)^{k-1} \times 10^3 \quad (5)$$

$$E_w = 3248.5 M_w \quad (6)$$

Where, P_w is the unit price of industrial distilled water.

3.4 Raw salt income

WSCPPDW can produce raw salt while generating freshwater. The income of raw salt in the k-th year can be expressed as follows:

$$B_s^k = E_s P_s (1 + \theta)^{k-1} \quad (7)$$

$$E_s = 3248.5 \eta_s E_w \times 10^3 \quad (8)$$

Where, η_s is the output efficiency of raw salt, $\eta_s = 3.5\%$; P_s is the unit price of raw salt.

4 Mathematical model of cost analysis

4.1 Integrated system construction cost

The construction cost of WSCPPDW mainly comes from the common chimney,

air turbine, heat collector, distillation tank, SGC, labor cost, material transportation cost, and the anticorrosion cost (flue inner wall of SGC, inner wall of common chimney and turbine blades surface). Besides, WSCPPDW chimney is made of high-performance concrete and rebar, and the hoisting cost of tall chimney accounts for 20% of the cost of concrete and rebar, excluding the transportation cost. The SGC is located below the ground level which is also made of concrete. Glass flake anticorrosive coating is applied to the common chimney inner wall and gas flue wall. The anticorrosive coating covers on the surface of turbine blades by plasma spraying based on the anticorrosive technology. If the transportation cost of materials accounts for 1.7% [42] of the material cost, the total cost and investment cost of WSCPPDW can be expressed as follows:

$$C_{tot} = 1.017C_{inv} \quad (9)$$

$$C_{inv} = C_{SGC} + C_{sys} + C_{anti} \quad (10)$$

Where, C_{SGC} is the cost of SGC; C_{sys} is the construction cost of other parts of WSCPPDW except SGC; C_{anti} is the anticorrosion cost of different parts in integrated system.

4.2 Interest cost

There are two common methods to repay the loan, one is the repayment of interest method, the other is the equal principal repayment method [39]. In order to reduce the cost of interest, this paper adopts the latter method. According to the working time of traditional thermal power plant, the loan of building WSCPPDW needs to be paid off within 30 years ($m=30$). The capital needed to be repaid in the k -th year can be expressed as follows:

$$C_{cap}^k = \frac{C_{tot}}{m} \quad (11)$$

The residual debt after repaying the capital and the interest in the k -th year can be respectively expressed as follows:

$$C_{debt}^k = C_{tot} - (k-1)C_{cap}^k \quad (12)$$

$$C_{int}^k = rC_{debt}^k \quad (13)$$

Where, r is the loan interest rate.

4.3 Tax cost

At the end of the working period of WSCPPDW, some components can be recycled, including support matrix, column structure, ring stiffener and so on. The net value of fixed assets and annual depreciation cost of the integrated system in the k -th year can be respectively expressed as follows:

$$C_{res}^k = C_{res}^{k-1}(1-d) \quad (14)$$

$$C_{depr}^k = C_{res}^k d \quad (15)$$

Where, d ($d=2/m$) is the double declining balance depreciation rate.

According to Chinese tax law, the depreciation expense and the loan interest can be excluded from the tax cost. The tax cost of the integrated system in the k -th year can be expressed as:

$$C_{tax}^k = (B_{all}^k - C_{int}^k - C_{depr}^k)t \quad (16)$$

Where, t is the income tax rate.

4.4 Operation and maintenance cost

The operating of WSCPPDW consumes labor cost, and the maintenance of heat collector, chimney, turbine and gas flue is also needed to be invested. In addition, the operation and maintenance cost is influenced by inflation rate. The operation and maintenance cost of the integrated system in the k -th year can be expressed as:

$$C_{O\&M}^k = C_{O\&M}^1 (1 + \varepsilon_{O\&M})^{k-1} \quad (17)$$

Where, $C_{O\&M}^1$ is the operation and maintenance cost of the first year [41], which is related to the power output of WSCPPDW; $\varepsilon_{O\&M}$ is the annual growth rate of operation and maintenance cost, which is considered to be equal to the inflation rate [41].

4.5 Insurance cost

The insurance cost of WSCPPDW includes the equipment loss and premium rate loss in the first year. It is assumed the total loss cost accounts for 0.8% of total investment [41]. The annual insurance cost is influenced by inflation rate. The insurance cost of WSCPPDW in the k-th year can be expressed as follows:

$$C_{insu}^k = C_{insu}^1 (1 + \theta)^{k-1} \quad (18)$$

$$C_{insu}^1 = 0.8\% C_{tot} \quad (19)$$

Where, C_{insu}^1 is the insurance cost in the first year.

5 Economic performance assessment

The total income and the total cost of WSCPPDW in the k-th year can be expressed as follows:

$$B_{all}^k = B_p^k + B_{CO_2}^k + B_w^k + B_s^k \quad (20)$$

$$C_{all}^k = C_{cap}^k + C_{int}^k + C_{O\&M}^k + C_{insu}^k \quad (21)$$

The annual net income (NET) and the total net income (TNET) of WSCPPDW in the k-th year can be respectively expressed as follows:

$$NET^k = B_{all}^k - C_{all}^k \quad (22)$$

$$TNET = \sum_{k=1}^m NET^k \quad (23)$$

In order to analyze the economic characteristic of WSCPPDW and SCPPDW, the annual cash flow during the working period need to be studied. The economic performance of the investment project depends on the discount rate to some extent. In this paper, the risk adjusted discount rate method is adopted. The discount rate can be expressed as follows:

$$x = \mu + yz \quad (24)$$

Where, μ , y and z represent risk-free discount rate, rate of risked return and risk degree, respectively.

The NPV and the total net present value (TNPV) of WSCPPDW in the k-th year can be expressed as follows:

$$NPV^k = \frac{(B_{all}^k - C_{all}^k)}{(1+x)^k} \quad (25)$$

$$TNPV = \sum_{k=1}^n NPV^k \quad (26)$$

Based on the working performance of WSCPPDW after orderly optimizing its turbine rotation speed, nozzle length, chimney outlet radius and mixing section length [17,35], the economic performance of the optimal WSCPPDW is studied. In the process of four-level optimization, the growth rate of annual NET and NPV in the k-th year relative to those of previous level can be expressed as follows:

$$\delta_{u+1} = \frac{NET_{u+1}^k - NET_u^k}{NET_u^k} \times 100\% \quad (27)$$

Where, u represents the optimization level, $0 \leq u \leq 4$. For example, NET_0^k is the annual NET in the k-th year with the initial parameters; NET_4^k is the annual NET in the k-th year after four-level optimization.

The economic parameters evolved in the cost-benefit analysis model are shown in Table 2.

Table 2 Economic parameters evolved in the economic analysis model.

Parameters	Symbol	Value
Inflation rate	θ	3%
Loan interest rate	r	3%
Income tax	t	13%
Annual growth rate	\mathcal{E}	3%
Discount rate	x	11.52%
Risk adjusted discount rate	μ	8%
Riskied return rate	y	8%
Risk degree	z	0.44
Double declining balance depreciation rate	d	1/15

6 Economic benefit analysis

6.1 Total income analysis

According to the references [17,51], the wind supercharging device installed at the chimney outlet could provide the negative pressure of 64.5 Pa. The power output and hourly freshwater yield of SCPPDW are 159.3 kW and 15.0 ton/h, respectively, and those of WSCPPDW are 193.7 kW and 17.2 ton/h, respectively. As shown in Fig.2 (a), under the effect of the wind supercharging device, the power output and hourly freshwater yield of WSCPPDW are increased by 21.6% and 14.7%, respectively. Fig.2 (b) shows the comparison of the TNET and TNPV in working period. It can be observed that, after adding the wind supercharging device at the chimney outlet, the TNET and TNPV of WSCPPDW are improved by 42.8% and 102.5%, respectively.

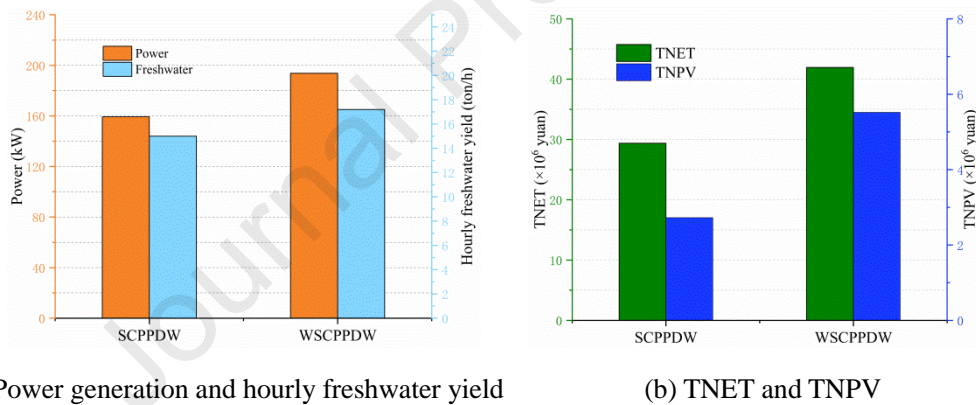


Fig.2 Performance parameters comparison of SCPPDW and WSCPPDW

6.2 Variation rules of economic performance

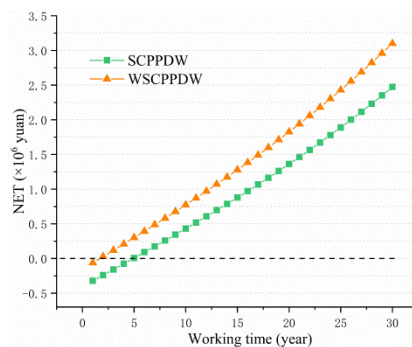


Fig.3 Annual NET variation rules of SCPPDW and WSCPPDW within the working period

Fig.3 shows the variation rule of the annual NET of SCPPDW and WSCPPDW.

It can be seen from Fig.3 that with the increasing of working years, the annual NET of SCPPDW and WSCPPDW increases gradually, and the annual NET of WSCPPDW is always larger than that of SCPPDW. The annual NET of SCPPDW is negative in the first four years and it is positive in the rest of working time. The annual NET of WSCPPDW is only negative in the first year.

This is because under the influence of inflation rate, with the increasing of working time, all of the electricity income, carbon credit income, freshwater income and raw salt income of SCPPDW and WSCPPDW increase year by year. In addition, because the fixed loan expense needs to be paid every year, both of the remaining loan and the annual loan interest decrease year by year. Therefore, the annual NET of SCPPDW and WSCPPDW increases year by year.

Fig.4 shows the NPV variation rules of SCPPDW and WSCPPDW within the working period. It can be seen from Fig. 4 that the NPV of SCPPDW increases first in the first 15 years and then decreases. It is negative in the first four years and positive in the rest of operating time. The NPV of WSCPPDW increases in the first 11 years and then decreases. It is only negative in the first year and it is always larger than the NPV of SCPPDW.

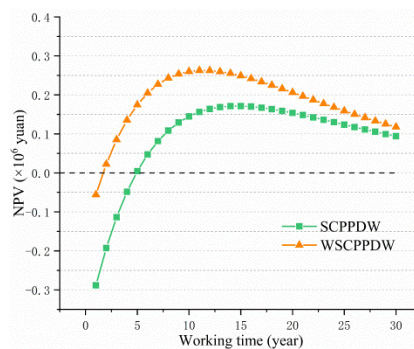


Fig.4 NPV variation rules of SCPPDW and WSCPPDW during the service period

This is because the annual NPV is mainly influenced by annual NET and discount rate. It can be known from Eq. (26) and (29) that NPV has a positive correlation with NET and has a negative correlation with discount rate. It is known from the above analysis that in the first 15 years, because the annual NET increases and the annual NET is the dominant factor affecting the change of NPV, the NPV of

SCPPDW increases. After 15 years, as the influence of discount rate becomes more significant, the NPV of SCPPDW decreases year by year. Similarly, the NPV of WSCPPDW increases first and then decreases. As shown in Fig.2, the power generation of WSCPPDW is obviously larger than that of SCPPDW. The annual operation and maintenance cost of WSCPPDW is higher than that of SCPPDW because of the positive correlation between operation and maintenance cost and power output. Because the annual operation and maintenance cost is inversely proportional to NPV, the inflection point of WSCPPDW where NPV starts to decrease is earlier than that of SCPPDW. In addition, because the annual NET of SCPPDW is negative in the first four years, its NPV is also negative. Because the annual NET of WSCPPDW is always larger than that of SCPPDW, the NPV of WSCPPDW is larger than that of SCPPDW.

6.3 The influence of the optimization of different parameters on the total income of integrated systems

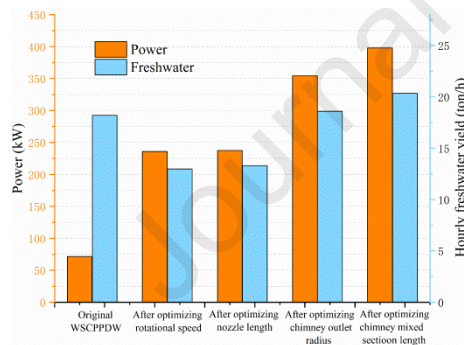


Fig.5 power and hourly freshwater yield

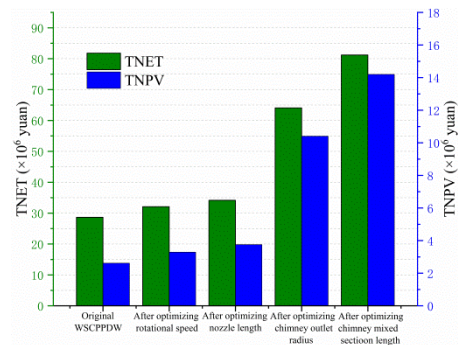


Fig.6 TNET and TNPV

Table 3 The parameters growth rate of each level optimization of WSCPPDW

Optimization parameters	Performance parameters			
	Power	Freshwater	TNET	TNPV
Rotational speed	222.7%	-28.6%	12.0%	25.9%
Nozzle length	2.8%	2.5%	6.5%	14.0%
Chimney outlet radius	33.9%	39.7%	87.5%	177.1%
Chimney mixing section length	25.1%	9.3%	26.8%	36.5%
Growth rate compared to the unoptimized system	455.8%	11.7%	183.4%	442.8%

According to our previous research results [35], the optimization of WSCPPDW was divided into four levels, that is, the optimization parameters of WSCPPDW, including the turbine rotational speed, nozzle length, chimney outlet radius and chimney mixing section length, are orderly optimized. The calculation of the optimization object of the latter level is based on the precondition that the optimization object of the former level has reached its optimal value. Fig.5 shows the power output and hourly freshwater yield of each level of sequential optimization of WSCPPDW. Fig.6 shows the TNET and TNPV of WSCPPDW under each level of sequential optimization. The optimization results of each level, including the growth rate of power output, growth rate of hourly freshwater yield, and TNET and TNPV of WSCPPDW, are shown in Table 3.

It can be seen from Table 3 that the power output significantly increases, and the hourly freshwater yield decreases after optimizing the turbine rotational speed. The optimization effect of nozzle length is not obvious, the power output and hourly freshwater yield are just slightly increased. The optimizations of turbine rotational speed and nozzle length both increase the TNET and TNPV of WSCPPDW. After optimizing the chimney outlet radius and the chimney mixing section length, all of the power generation, the hourly freshwater production, TNET and TNPV are significantly increased. After the four-level optimization, compared with those of the original system without any optimization, the power generation and hourly freshwater production are increased by 455.8% and 11.7%, respectively, and the TNET and TNPV are increased by 183.4% and 442.8%, respectively.

6.4 The influence of different optimization parameters on the annual change of economic performance of WSCPPDW

Fig. 7 shows the annual NET and NPV change curves year by year after sequentially optimizing the turbine rotational speed, nozzle length, chimney outlet radius and mixing section length of WSCPPDW. Table 4 shows the increase rate and growth rate of annual NET and NPV after the sequential optimization.

As shown in Fig.7 and Table 4, in the process of sequential optimization of turbine rotational speed, nozzle length, chimney outlet radius and mixing section length of WSCPPDW, both of the annual NET and NPV are increased. After optimizing the turbine rotational speed and nozzle length, the annual NET and NPV are only increased slightly. After optimizing the chimney outlet radius and the mixing section length, the annual NET and NPV are significantly increased. After optimizing the chimney outlet radius, the growth of annual NET and NPV is the largest, and the average annual rises are 9.97×10^5 yuan and 2.217×10^5 yuan, respectively. After four-level optimization, the annual NET and NPV of WSCPPDW are averagely increased by 2.4×10^6 yuan and 3.9×10^5 yuan, respectively. It can be seen from the above that the optimization of different parameters of WSCPPDW improves power output and hourly freshwater yield, which further increases the annual NET and NPV. Because the power generation is obviously increased and the freshwater production is decreased, the annual NET and NPV of WSCPPDW only increase slightly after optimizing the turbine rotational speed.

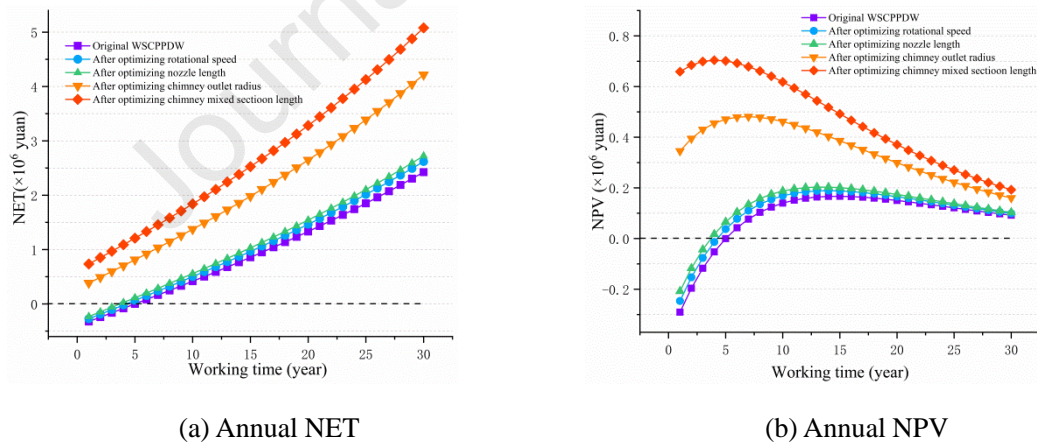


Fig.7 The annual NET and NPV change curves of WSCPPDW.

As shown in Fig. 7 (a) and (b), with the increasing of working time of WSCPPDW, its annual NET increases year by year, and the annual NPV increases first and then decreases. In the process of four-level optimization, the inflection points of NPV appear in the 14th, 13th, 7th and 4th year, respectively. The declining inflection point of annual NPV is brought forward by 10 years after four-level

optimization.

It can be seen from the above that influenced by inflation rate, the annual NET of WSCPPDW increases year by year. Therefore, as the working time gets longer, the annual NPV increases year by year. With the further increase of working time, the influence of the discount rate on NPV becomes more and more significant, thus the annual NPV decreases yearly. After each level optimization, the operation and maintenance cost of WSCPPDW is significantly increased, and the declining inflection point of annual NPV is much earlier due to the obvious increase of power output.

It can be seen from Table 4 that with the increasing of working time, the growth value of NET between two adjacent optimization levels is improved continually, and the growth value of NPV decreases between two layers decreases. The growth rate of NET between adjacent optimization levels is equal to that of NPV according to Eq. (25) and (27). Before optimizing the chimney mixing section length (the fourth level), the growth rate increases first and then decreases. And it decreases continually after optimizing the chimney mixing section length.

This is because the benefit from optimizing WSCPPDW parameters is larger than the paid cost, the NET growth value increases continually. Under the effects of discount rate, which effect becomes larger with the increase of working time, the NPV growth value decreases according to Eq. (25). The NET of WSCPPDW with initial design parameters is negative in the first five years. Then, after optimizing the turbine rotational speed (the first level) and nozzle length (the second level), the NETs of WSCPPDW are negative in the first four years and the first three years, respectively. For the optimization results of the first three levels, as the working time gets longer, their growth rates are improved to very large values. Because the denominator (the NET of the previous optimization level) is approaching to zero from a negative value, the growth rate of NPV will become extremely large, according to Eq. (27). With the further increasing of working time, the growth rate of NPV decreases under the effects

of inflation rate. For the optimization result of the fourth level (the chimney mixing section length), the growth rate reduces continually, because the annual NET in the third level (the chimney outlet radius) is always positive and increases continually.

Table 4 The growth of annual NET and NPV after sequential optimization.

Working duration (year)	Optimize rotational speed			Optimize nozzle length		
	Growth of NET (million)	Growth of NPV (million)	Growth rate (%)	Growth of NET (million)	Growth of NPV (million)	Growth rate (%)
1	0.0497	0.0445	15.3150	0.0428	0.0384	15.5819
2	0.0533	0.0429	21.8971	0.0442	0.0355	23.2069
3	0.0571	0.0412	35.0638	0.0456	0.0329	43.0986
4	0.0609	0.0394	74.5082	0.0470	0.0304	225.6766
5	0.0648	0.0376	25759.4925	0.0485	0.0281	75.1949
6	0.0687	0.0357	84.0759	0.0501	0.0260	33.2714
7	0.0727	0.0339	44.2656	0.0516	0.0241	21.7849
8	0.0768	0.0321	31.0312	0.0533	0.0223	16.4206
9	0.0810	0.0304	24.4254	0.0549	0.0206	13.3161
10	0.0853	0.0287	20.4686	0.0567	0.0190	11.2935
11	0.0896	0.0270	17.8357	0.0584	0.0176	9.8724
12	0.0940	0.0254	15.9590	0.0603	0.0163	8.8200
13	0.0986	0.0239	14.5549	0.0621	0.0151	8.0101
14	0.1032	0.0224	13.4658	0.0641	0.0139	7.3681
15	0.1080	0.0210	12.5971	0.0661	0.0129	6.8471
16	0.1128	0.0197	11.8887	0.0681	0.0119	6.4163
17	0.1178	0.0185	11.3006	0.0702	0.0110	6.0544
18	0.1228	0.0173	10.8050	0.0724	0.0102	5.7465
19	0.1281	0.0161	10.3821	0.0746	0.0094	5.4816
20	0.1334	0.0151	10.0173	0.0769	0.0087	5.2514
21	0.1388	0.0141	9.6998	0.0793	0.0080	5.0498
22	0.1444	0.0131	9.4211	0.0817	0.0074	4.8720
23	0.1502	0.0122	9.1749	0.0842	0.0069	4.7140
24	0.1561	0.0114	8.9560	0.0868	0.0063	4.5730
25	0.1621	0.0106	8.7603	0.0895	0.0059	4.4465
26	0.1683	0.0099	8.5845	0.0922	0.0054	4.3324
27	0.1747	0.0092	8.4259	0.0951	0.0050	4.2292
28	0.1812	0.0086	8.2823	0.0980	0.0046	4.1355
29	0.1879	0.0080	8.1517	0.1009	0.0043	4.0501
30	0.1947	0.0074	8.0326	0.1040	0.0039	3.9720
Average value	0.1146	0.0226		0.0693	0.0154	

Working duration (year)	Optimize chimney outlet radius			Optimize chimney mixing section length		
	Growth of NET (million)	Growth of NPV (million)	Growth rate (%)	Growth of NET (million)	Growth of NPV (million)	Growth rate (%)
1	0.6173	0.5535	266.3067	0.3491	0.3130	90.5667
2	0.6369	0.5121	435.8704	0.3607	0.2900	73.4937
3	0.6571	0.4738	1092.1335	0.3726	0.2686	62.4174
4	0.6779	0.4383	2588.4973	0.3848	0.2488	54.6567
5	0.6992	0.4054	618.5416	0.3974	0.2304	48.9214
6	0.7212	0.3749	359.6904	0.4103	0.2133	44.5140
7	0.7438	0.3467	257.6654	0.4236	0.1975	41.0240
8	0.7671	0.3207	203.1216	0.4372	0.1828	38.1945
9	0.7911	0.2965	169.1966	0.4513	0.1692	35.8562
10	0.8157	0.2742	146.0761	0.4657	0.1565	33.8932
11	0.8411	0.2535	129.3217	0.4806	0.1448	32.2234
12	0.8672	0.2344	116.6331	0.4959	0.1340	30.7869
13	0.8941	0.2167	106.6992	0.5116	0.1240	29.5392
14	0.9218	0.2003	98.7180	0.5278	0.1147	28.4464
15	0.9503	0.1852	92.1712	0.5445	0.1061	27.4822
16	0.9796	0.1712	86.7091	0.5616	0.0981	26.6260
17	1.0098	0.1582	82.0870	0.5793	0.0908	25.8614
18	1.0408	0.1462	78.1289	0.5974	0.0839	25.1751
19	1.0728	0.1352	74.7046	0.6161	0.0776	24.5562
20	1.1058	0.1249	71.7159	0.6353	0.0718	23.9959
21	1.1397	0.1154	69.0874	0.6551	0.0664	23.4867
22	1.1746	0.1067	66.7599	0.6755	0.0614	23.0225
23	1.2105	0.0986	64.6868	0.6965	0.0567	22.5980
24	1.2476	0.0911	62.8305	0.7180	0.0524	22.2086
25	1.2857	0.0842	61.1605	0.7403	0.0485	21.8507
26	1.3249	0.0778	59.6517	0.7631	0.0448	21.5209
27	1.3653	0.0719	58.2833	0.7867	0.0414	21.2163
28	1.4069	0.0664	57.0381	0.8109	0.0383	20.9346
29	1.4498	0.0614	55.9015	0.8359	0.0354	20.6735
30	1.4939	0.0567	54.8610	0.8616	0.0327	20.4311
Average Value	0.9970	0.2217		0.5715	0.1265	

7 Conclusions

In this paper, in order to research the economic performance of SCPPDW and WSCPPDW, an economic analysis model is developed. Based on NPV method, the

economic performance of SCPPDW and WSCPPDW and their economic characteristics after sequentially optimizing working and geometric parameters are studied. The main conclusions are as follows:

(1) After adding the wind supercharging device at the chimney outlet, the TNET and TNPV of WSCPPDW are increased by 42.8% and 102.5%, respectively. As the working time gets longer, the annual NET of two integrated systems shows increasing trend. The annual NPV of SCPPDW and WSCPPDW increases first and then decreases, and the maximum values appear in the 15th and 11th year, respectively. The annual NET and NPV of WSCPPDW are always larger than those of SCPPDW. Those of SCPPDW are negative in the first four years, and those of WSCPPDW are only negative in the first year.

(2) The power output significantly increases, and the hourly freshwater yield decreases after optimizing the turbine rotational speed of WSCPPDW. The optimization effect of nozzle length is not obvious, the power generation and hourly freshwater production are just slightly improved. The optimizations of turbine rotational speed and nozzle length both improve the TNET and TNPV. After optimizing the chimney outlet radius and the chimney mixing section length, all of the power generation, hourly freshwater production, TNET and TNPV are significantly increased. After four-level optimization (turbine rotational speed, nozzle length, chimney outlet radius and mixing section length), compared with the initial WSCPPDW, the power output and the hourly freshwater yield are increase by 455.8% and 11.7%, respectively, and the TNET and TNPV are improved by 183.4% and 442.8%, respectively.

(3) In the process of four-level sequential optimization, the annual NET and NPV both increase after optimizing each level parameters. After optimizing the turbine rotational speed and nozzle length, the annual NET and NPV only are increased slightly. After optimizing the chimney outlet radius and the mixing section length, the annual NET and NPV are increased significantly. After four-level optimization, the

annual NET and NPV of WSCPPDW are averagely improved by 2.4×10^6 yuan and 3.9×10^5 yuan, respectively.

(4) As the working time of WSCPPDW gets longer, the annual NET increases and the annual NPV firstly increases and then decreases. The inflection point of annual NPV is brought forward by 10 years after fourth-level optimization. Before optimizing the chimney mixing section length, the growth rates of annual NET and NPV both increase and then decrease. After optimizing the chimney mixing section length, the growth rates of annual NET and NPV decrease continually.

Symbol table

Letter

B	Benefit (yuan)
C	Cost (yuan)
D	Double declining balance depreciation rate (%)
E	Annual output
k	The k-th year
m	Total years of working (year), m=30
M	Freshwater output (ton)
NET	Net income (yuan)
NPV	Net present value (yuan)
p	Power (kW)
r	Loan rate (%)
TNET	Total net income (yuan)
TNPV	Total net present value (yuan)
V	Volume of construction material (m^3)
x	The discount rate
y	The rate of risked return
z	The risk degree

Subscripts

all	Total income or total cost
anti	Anticorrosion
cap	Capital

CO ₂	Carbon emission
debt	Debt
depr	Annual depreciation expense
insu	Insurance
int	Interest
inv	Investment
O&M	Operation and maintenance cost
p	Unit price
res	Net value of fixed assets
s	Raw salt
sys	System
t	Income tax rate
tax	Tax
tot	The integrated system
u	The u-th optimization
w	Freshwater
<i>Greek symbol</i>	
θ	Inflation rate
η_s	Output efficiency of raw salt, $\eta_s=3.5\%$
ε	Annual growth rate
μ	The risk-free discount rate
δ	The growth rate of annual NET and NPV

Acknowledgment

This research is financially supported by National Natural Science Foundation of China (No. 51976053) and College Students Innovation and Entrepreneurship Training Program of Hohai University (No. 202010294034).

Reference

- [1] Robert R. Spanish solar chimney nears completion. *MPS Review* 1981;6:21–3.
- [2] Haaf W, Friedrich K, MAYR G, Schlaich J. Part I: Principle and Construction of the Pilot Plant in Manzanares. *International Journal of Solar Energy* 1983;2:3–20. <https://doi.org/10.1080/01425918308909911>.

- [3] Haaf W. Solar Chimney, Part II: Preliminary test results from the manzanares pilot plant. *Solar Energy* 1984;2:41–61.
- [4] J S. The Solar Chimney. *Energy* 2002:1–14.
- [5] Trieb F, Langniß O, Klaiß H. Solar electricity generation-A comparative view of technologies, costs and environmental impact. *Solar Energy* 1997;59:89–99. [https://doi.org/10.1016/S0038-092X\(97\)80946-2](https://doi.org/10.1016/S0038-092X(97)80946-2).
- [6] Gannon AJ, Von Backström TW. Solar chimney cycle analysis with system loss and solar collector performance. *Journal of Solar Energy Engineering* 2000;122:133–7. <https://doi.org/10.1115/1.1314379>.
- [7] Pan Yuan, Gu Chenglin, Zhou Libing, Wei Jun, Huang Shenghua, Li Langru, Ma Zhiyun. The generation of electricity by solar hot air-flows and its effect on China's energy sources and environment. *International Journal World Sci-Tech R&D*, 2003;25(4): 7-12.
- [8] Ge X., Ye H. Solar chimney electric generating system and analysis of its intrinsic thermodynamic defect. *Acta Energetica Solaris Sinica*, 2004;25(2):263-8.
- [9] Guo PH, Li JY, Wang Y. Annual performance analysis of the solar chimney power plant in Sinkiang, China. *Energy Conversion and Management* 2014;87:392–9. <https://doi.org/10.1016/j.enconman.2014.07.046>.
- [10] Khanal R, Lei C. Solar chimney-A passive strategy for natural ventilation. *Energy Buildings* 2011;43:1811–9. <https://doi.org/10.1016/j.enbuild.2011.03.035>.
- [11] Ho CJ, Chou WL, Lai CM. Thermal and electrical performances of a water-surface floating PV integrated with double water-saturated MEPCM layers. *Applied Thermal Engineering* 2016;94:122–32. <https://doi.org/10.1016/j.applthermaleng.2015.10.097>.
- [12] Zuo Lu, Yuan Yue, Li Zhenjie, Zheng Yuan. Experimental research on solar chimneys integrated with seawater desalination under practical weather condition. *Desalination* 2012;298:22–33. <https://doi.org/10.1016/j.desal.2012.05.001>.
- [13] Kiwan S, Al-Nimr M, Abdel Salam QI. Solar chimney power-water distillation plant (SCPWDP). *Desalination* 2018;445:105–14. <https://doi.org/10.1016/j.desal.2018.08.006>.
- [14] Ming T, Gong T, de Richter RK, Cai C, Sherif SA. Numerical analysis of seawater desalination based on a solar chimney power plant. *Applied Energy* 2017;208:1258–73. <https://doi.org/10.1016/j.apenergy.2017.09.028>.
- [15] Asayesh M, Kasaean A, Ataei A. Optimization of a combined solar chimney for desalination and power generation. *Energy Conversion and Management* 2017;150:72–80. <https://doi.org/10.1016/j.enconman.2017.08.006>.
- [16] Lu Zuo, Zihan Liu, Xiaotian Zhou, Ling Ding, Jiajun Chen, Ning Qu, Yue Yuan. Preliminary study of wind supercharging solar chimney power plant combined with seawater desalination by indirect condensation freshwater production. *Desalination* 2019;455:79–88. <https://doi.org/10.1016/j.desal.2019.01.008>.
- [17] Lu Zuo, Zihan Liu, Ling Ding, Ning Qu, Pengzhan Dai, Bofeng Xu, Yue Yuan. Performance analysis of a wind supercharging solar chimney power plant combined with thermal plant for power and freshwater generation. *Energy Conversion and Management* 2020;204:112282. <https://doi.org/10.1016/j.enconman.2019.112282>.
- [18] Yiping Wang, Junhong Wang, Li Zhu, Zhiyong Yang, Zhenlei Fang. The study of sea

- desalination and hot wind electric power integrated system by solar chimney. *Acta Energiæ Solaris Sinica* 2006;27:731–6.
- [19] Yiping Wang, Zhenlei Fang, Li Zhu, Zhiyong Yang, Junhong Wang, Lijun Han. Study on the integrated utilization of seawater by solar chimney. *Acta Energiæ Solaris Sinica* 2006;27:382–7.
- [20] Zhu Li, Wang Junhong, Wang Yiping, Yang Zhiyong, Fang Zhenlei. Seawater Desalination and Waterpower Integrated System with Solar Chimney. *Journal of Tianjin University* 2006;39:575–80.
- [21] Taylor P, Vlachos NA, Karapantsios TD, Balouktsis AI, Chassapis D. Design and testing of a new solar tary dryer. *Drying Technology* 2002;20(6);1241-71.
- [22] Al-Kayiem HH, Aja OC. Historic and recent progress in solar chimney power plant enhancing technologies. *Renewable Sustainable Energy Review* 2016;58:1269–92. <https://doi.org/10.1016/j.rser.2015.12.331>.
- [23] Al-Kayiem HH, Yin Yin K, Yee Sing C. Numerical simulation of solar chimney integrated with exhaust of thermal power plant. *WIT Transactions on Engineering Sciences* 2012;75:61–72. <https://doi.org/10.2495/HT120061>.
- [24] Ghorbani B, Ghashami M, Ashjaee M. Electricity production with low grade heat in thermal power plants by design improvement of a hybrid dry cooling tower and a solar chimney concept. *Energy Conversion and Management* 2015;94:1–11. <https://doi.org/10.1016/j.enconman.2015.01.044>.
- [25] Aurybi MA, Al-Kayiem HH, Gilani SIU, Ismaeel AA. Numerical assessment of solar updraft power plant integrated with external heat sources. *WIT Transactions on Ecology and The Environment* 2017;226:657–66. <https://doi.org/10.2495/SDP170571>.
- [26] Mann HS, Singh PK. Conceptual development of an energy recovery from the chimney flue gases using ducted turbine system. *Journal of Natural Gas Science and Engineering* 2016;33:448–57. <https://doi.org/10.1016/j.jngse.2016.05.044>.
- [27] Aurybi MA, Gilani SI, Al-Kayiem HH, Ismaeel AA. Mathematical evaluation of solar chimney power plant collector, integrated with external heat source for non-interrupted power generation. *Sustainable Energy Technologies and Assessments* 2018;30:59–67. <https://doi.org/10.1016/j.seta.2018.06.012>.
- [28] Al-Kayiem HH, Aurybi MA, Gilani SIU, Ismaeel AA, Mohammad ST. Performance evaluation of hybrid solar chimney for uninterrupted power generation. *Energy* 2019;166:490–505. <https://doi.org/10.1016/j.energy.2018.10.115>.
- [29] Hu S, Leung DYC. Numerical Modelling of the Compressible Airflow in a Solar-Waste-Heat Chimney Power Plant. *Energy Procedia* 2017;142:642–7. <https://doi.org/10.1016/j.egypro.2017.12.106>.
- [30] Habibollahzade A, Houshfar E, Ashjaee M, Behzadi A, Gholamian E, Mehdizadeh H. Enhanced power generation through integrated renewable energy plants: Solar chimney and waste-to-energy. *Energy Conversion and Management* 2018;166:48–63. <https://doi.org/10.1016/j.enconman.2018.04.010>.
- [31] Habibollahzade A, Houshfar E, Ahmadi P, Behzadi A, Gholamian E. Exergoeconomic assessment and multi-objective optimization of a solar chimney integrated with

- waste-to-energy. *Solar Energy* 2018;176:30–41. <https://doi.org/10.1016/j.solener.2018.10.016>.
- [32] Shahreza AR, Imani H. Experimental and numerical investigation on an innovative solar chimney. *Energy Conversion and Management* 2015;95:446–52. <https://doi.org/10.1016/j.enconman.2014.10.051>.
- [33] Attig-Bahar F, Sahraoui M, Guellouz MS, Kaddeche S. Effect of the ground heat storage on solar chimney power plant performance in the South of Tunisia: Case of Tozeur. *Solar Energy* 2019;193:545–55. <https://doi.org/10.1016/j.solener.2019.09.058>.
- [34] Joneydi Shariatzadeh O, Refahi AH, Abolhassani SS, Rahmani M. Modeling and optimization of a novel solar chimney cogeneration power plant combined with solid oxide electrolysis/fuel cell. *Energy Conversion and Management* 2015;105:423–32. <https://doi.org/10.1016/j.enconman.2015.07.054>.
- [35] Zuo, Lu, Dai Pengzhan, Liu Zihan, Qu Ning, Ding Ling, Qu Bo, Yuan Yue. Numerical analysis of wind supercharging solar chimney power plant combined with seawater desalination and gas waste heat. *Energy Conversion and Management* 2020;223:113250. <https://doi.org/10.1016/j.enconman.2020.113250>.
- [36] Bernardes MA dos S. Technische, ökonomische und ökologische Analyse von Aufwindkraftwerken 2004:230.
- [37] Schlaich J, Bergermann R, Schiel W, Weinrebe G. Design of commercial solar updraft tower systems - Utilization of solar induced convective flows for power generation. *Journal Solar Energy Engineering* 2005;127:117–24. <https://doi.org/10.1115/1.1823493>.
- [38] Nizetic S, Ninic N, Klarin B. Analysis and feasibility of implementing solar chimney power plants in the Mediterranean region. *Energy* 2008;33:1680–90. <https://doi.org/10.1016/j.energy.2008.05.012>.
- [39] Zhou X, Yang J, Wang F, Xiao B. Economic analysis of power generation from floating solar chimney power plant. *Renewable Sustainable Energy Review* 2009;13:736–49. <https://doi.org/10.1016/j.rser.2008.02.011>.
- [40] Fluri TP, Pretorius JP, Dyk C Van, Von Backström TW, Kröger DG, Zijl GPAGV. Cost analysis of solar chimney power plants. *Solar Energy* 2009;83:246–56. <https://doi.org/10.1016/j.solener.2008.07.020>.
- [41] Cao F, Li H, Zhao L, Guo L. Economic analysis of solar chimney power plants in Northwest China. *Renewable and Sustainable Energy Reviews* 2013;5(2):021406. <https://doi.org/10.1063/1.4798434>.
- [42] Li W, Wei P, Zhou X. A cost-benefit analysis of power generation from commercial reinforced concrete solar chimney power plant Weibing. *Energy Conversion and Management* 2014;79:104–13. <https://doi.org/10.1016/j.enconman.2013.11.046>.
- [43] Akhtar Z. Study of economic viability of 200 MW solar chimney power plant in Rajasthan, India 2014:84–8.
- [44] Gholamalizadeh E, Kim MH. Thermo-economic triple-objective optimization of a solar chimney power plant using genetic algorithms. *Energy* 2014;70:204–11. <https://doi.org/10.1016/j.energy.2014.03.115>.
- [45] Okoye CO, Atikol U. A parametric study on the feasibility of solar chimney power plants

- in North Cyprus conditions. *Energy Conversion and Management* 2014;80:178–87. <https://doi.org/10.1016/j.enconman.2014.01.009>.
- [46] Okoye CO, Solyali O, Taylan O. A new economic feasibility approach for solar chimney power plant design. *Energy Conversion and Management* 2016;126:1013–27. <https://doi.org/10.1016/j.enconman.2016.08.080>.
- [47] Ali B. Techno-economic optimization for the design of solar chimney power plants. *Energy Conversion and Management* 2017;138:461–73. <https://doi.org/10.1016/j.enconman.2017.02.023>.
- [48] Penghau Guo, Yaxin Zhai, Xinhai Xu, Jingyin Li. Assessment of levelized cost of electricity for a 10-MW solar chimney power plant in Yinchuan China. *Energy Conversion and Management* 2017;152:176–85. <https://doi.org/10.1016/j.enconman.2017.09.055>.
- [49] Jamali S, Nemati A, Mohammadkhani F, Yari M. Thermal and economic assessment of a solar chimney cooled semi-transparent photovoltaic (STPV) power plant in different climates. *Solar Energy* 2019;185:480–93. <https://doi.org/10.1016/j.solener.2019.04.073>.
- [50] Lu Zuo, Ning Qu, Zihan Liu, Ling Ding, Pengzhan Dai, Bofeng Xu, Yue Yuan. Performance study and economic analysis of wind supercharged solar chimney power plant. *Renewable Energy* 2020;156:837–50. <https://doi.org/10.1016/j.renene.2020.04.032>.
- [51] Lu Zuo, Ling Ding, Jiajun Chen, Xiaotian Zhou, Bofeng Xu, Zihan Liu. Comprehensive study of wind supercharged solar chimney power plant combined with seawater desalination. *Solar Energy* 2018;166:59–70. <https://doi.org/10.1016/j.solener.2018.03.041>.

Highlights:

- The economic analysis model of WSCPPDW was developed.
- The effect of wind supercharging device on economic performance of WSCPPDW was studied.
- The influence of the optimization of different parameters on economic performance was explored.
- The annual change regulations of economic performance of WSCPPDW were researched.

Declaration of interests

The authors declare that they have no known competing financial interests or personal relationships that could have appeared to influence the work reported in this paper.

The authors declare the following financial interests/personal relationships which may be considered as potential competing interests:

Journal Pre-proof

Credit Author Statement

The division of labor among the authors is shown as bellow:

Lu Zuo:	Conceptualization, methodology, supervision, project administration, funding acquisition.
Zihan Liu:	Software, formal analysis, validation, investigation, writing-original draft.
Pengzhan Dai:	Data curation
Ning Qu:	Visualization
Ling Ding:	Resources
Yuan Zheng:	Writing-Review & Editing
Yunting Ge:	Research methods and data analysis guidance